JOURNAL OF CATALYSIS 80, 286–295 (1983)

Low Energy Ion Scattering Study of Ni-Mo–Al_2O_3 Catalysts

HELGE JEZIOROWSKI,*,[1] HELMUT KNÖZINGER,*,[2] EDMUND TAGLAUER,† AND CLAUS VOGDT*

*Institut für Physikalische Chemie, Universität München, Sophienstrasse 11, 8000 München 2, and †Max-Planck-Institut für Plasmaphysik, Euratom-Association, 8046 Garching, West Germany

Received July 13, 1982

The principles of low energy ion scattering (ISS) and its application to the study of real catalyst surfaces are discussed. As a special example, the effect of the calcination temperature of a Ni-Mo/Al_2O_3 on the elemental distribution is studied. From the ISS "depth profiles" it can be concluded that at temperatures <770 K the molybdate phase on the Al_2O_3 support forms islands with three-dimensional extension while uncovered support surface remains even though the loading corresponds to the theoretical monolayer capacity. A spreading of the molybdate over the support surface occurs at 870 K to form a more or less closed monolayer. Simultaneously, Ni^{2+} ions are lost from the surface molybdate by penetration into subsurface layers of the Al_2O_3 matrix where they occupy octahedral and tetrahedral sites. The importance of the redistribution of promotor ions and the dispersion of the molybdate phase for the catalytic performance is emphasized.

INTRODUCTION

Low energy ion scattering (ISS) has been known as a surface sensitive technique since more than one decade (*1–3*). Nevertheless, the method has been applied for the characterization of practical catalysts in only a few cases up to now. Shelef *et al.* (*4*) were the first to study by ISS the surface composition and the elemental depth distribution of various transition metal aluminates in relation to their chemisorption properties. Brongersma *et al.* (*5*) studied the effect of Mo or Bi enrichment on the surface composition of Bi_2MoO_6 catalysts. The number of published papers on ISS studies of practical catalysts increased only during the last 2 years. Nickel/alumina and cobalt/alumina catalysts were subjects for the work of Hercules and his co-workers (*6–8*). Particularly attractive for characterization by ISS are the unpromoted and promoted monolayer-type catalysts such as molybdenum/alumina catalysts. They have in fact found increasing interest. Thus, Zingg *et al.* (*9*) have demonstrated the usefulness of the combined application of the ISS method together with X-ray photoelectron and Raman spectroscopy for the physical characterization of a molybdena/alumina catalyst. Delannay *et al.* (*10, 11*) were able to lend support toward the previously suggested (*12*) Co-Mo double layer structure of $CoMo/\gamma\text{-}Al_2O_3$ catalysts. For the $NiMo/\gamma\text{-}Al_2O_3$ system we could demonstrate (*13–16*) that the Ni atoms in this catalyst are located within the surface molybdate layer and in the $\gamma\text{-}Al_2O_3$ support but an enrichment of Ni at the interface between molybdate layer and support could not be detected.

It is the purpose of the present paper to demonstrate the usefulness of this technique for the analysis of the surface elemental composition and the depth distribution of practical catalysts even though their surfaces are normally rather badly defined geometrically and though they are porous. Again the $NiMo/\gamma\text{-}Al_2O_3$ system has been chosen and it will be shown how calcination temperature influences surface composition, depth distribution, and structure of the active phase. In order to complement

[1] Present address: WIM, Erding bei München, West Germany.

[2] To whom all correspondence should be addressed.

0021-9517/83 $3.00

the ISS data and to support the conclusions drawn therefrom other physical techniques, namely Raman and optical spectroscopy and magnetic susceptibility measurements, have also been applied.

Physical Background of the ISS Technique

The technique is not well known among catalyst chemists and therefore some introduction is appropriate. It consists in measuring the residual energy of the ions in a well-defined beam after scattering from the surface of a solid. This energy spectrum is equivalent to a mass spectrum of the surface atoms, since it represents the energy transfers which take place in single collisions between the ions and the surface atoms:

$$\frac{E}{E_0} = \frac{M_0^2}{(M_0 + M_s)^2} \left[\cos\theta + \left(\frac{M_s^2}{M_0^2} - \sin\theta\right)^{1/2}\right]^2, \quad (1)$$

for $M_s > M_0$,

where E_0 and E are the kinetic energies of the primary and backscattered ions, respectively, M_s is the mass of a surface atom, and θ the scattering angle relative to the direction of the incident ion beam. It is clear from this relation that well-defined monoenergetic (energy spread $\leq$10 eV for E_0 = 1000 eV) and well collimated (angular spread $\geq 1°$) ion beams are required to achieve optimum resolution.

In contrast to other surface science techniques such as Auger electron and X-ray photoelectron spectroscopy which have a finite electron energy dependent information depth, ISS has the particular attraction of providing a probing depth of one atomic layer (*17*), i.e., only ions backscattered from the topmost atomic layer are detected and convey information on the masses and abundance of atoms in this layer. This extreme surface sensitivity of ISS is due to two factors, namely the relatively large scattering cross-sections and the neutralization effect.

Differential scattering cross-sections $d\sigma/d\Omega$ can be calculated using theoretical or semi-empirical interaction potentials. Reasonable values which are in good agreement with experimental data are obtained from a screened Coulomb potential

$$V\left(\frac{r}{a}\right) = \frac{Z_0 Z_s e^2}{r} \Phi\left(\frac{r}{a}\right) \quad (2)$$

using the Molière approximation for the screening function $\Phi(r/a)$ (*17*). In Eq. (2), Z_0 and Z_s are the atomic numbers of the incident ion and the surface atom, respectively, and r is their distance. The screening parameter a is usually chosen according to Firsov (*18*) and designated a_F; better agreement with experimental results, however, is obtained for $a = 0.8\ a_F$ (*19, 20*). Some values of differential scattering cross sections $d\sigma/d\Omega$ relevant to the present study are summarized in Table 1 for a scattering angle of 137° (used in the experimental work) and primary energies of $^4He^+$ ions of 500 and 2000 eV. It can be seen from Table 1 that the scattering cross sections increase with increasing mass M_s of the surface atom particularly for low atomic masses ($M_s <$ 30) and that scattering cross sections are significantly higher for lower primary energies. Hence, monolayer specificity will be enhanced for low primary energies.

In ISS only backscattered positive ions are analyzed. Thus, primary ions which are neutralized during the scattering process do not contribute to the signal. It has been established that neutralization is particularly

TABLE 1

Differential Scattering Cross Sections (Å²/sr) for $^4He^+$ at a Scattering Angle of 137°

	500 eV	2000 eV
$He^+ \rightarrow O$	3.31×10^{-3}	4.85×10^{-4}
$He^+ \rightarrow Al$	6.07×10^{-3}	1.04×10^{-4}
$He^+ \rightarrow Ni$	1.26×10^{-2}	2.70×10^{-3}
$He^+ \rightarrow Mo$	1.74×10^{-2}	4.07×10^{-3}

effective for those ions which penetrate below the first atomic layer into the sample and undergo multiple collisions (*17*). This is certainly true for primary ion energies of about 500 eV or less. For higher energies (~2000 eV and higher) multiple collision effects are observed as background intensity on the low energy flank of the main peaks. For all these reasons we have used $^4He^+$ ions with a primary energy of 500 eV in the experimental work in contrast to most other workers.

The probability that the primary ion survives in its ionic state during the collision process is of the order of 1 to 10% in the energy range below 2000 eV; its exact value, however, is generally not known. It has been shown that the neutralization probability is most probably an atomic property (*21*), i.e., it only depends on the nature of the scattering atom irrespective of its chemical environment, if the incidence and exit angles are close (~30°) to the surface normal. This approach seems to be most commonly and successfully used. One usual way to cope with the problem of unknown neutralization probabilities is to consider only intensity ratios, which provide values which are proportional to the relative abundance of several elements. The only assumption made in this approach is that the neutralization probabilities for the considered elements do not change during the experiment (e.g., depth profiling). According to all present experience this assumption is justified.

Depth distributions of atoms in the catalyst surface can be determined by sputter etching. For this purpose the primary ion beam can be used and energy spectra taken at increasing bombardment times can then in principle be converted into concentration depth profiles for geometrically flat surfaces. To avoid a possible so-called "crater-effect" connected with the approximately Gaussian density profile of the ion beam, two techniques can be applied: (a) rastergating, i.e., spectra are only taken when the ion beam hits the central part of a rastered area (*22*), or (b) applying different beam diameters on the surface for the etching (e.g., 1 mm) and analyzing (e.g., 0.2 mm) beams. In presently known studies on real catalyst surfaces which deal with this problem (*10, 14, 15*), the possible crater effect did not seem to have posed major problems.

Samples of practical catalysts are usually prepared as pressed wafers, the geometric surface of which consists of densely packed, irregularly formed, and porous particles. The angle of incidence of the ion beam therefore varies over the sputtered area; hence, an ideal layer-by-layer erosion during sputtering is impossible. Sputtering rates are known to depend markedly on the angle of incidence with a maximum near 10 to 30° relative to the surface (*23, 24*), so that homogeneous erosion cannot be expected for disperse samples. Nevertheless, at least concentration ratios taken at zero bombardment time provide extremely useful information. Also spectra recorded within the average time for erosion of a monolayer should give significant qualitative information on changes of concentration ratios between the topmost and the next few atomic layers, although these data taken at a certain sputtering time can certainly not be attributed to a well-defined depth. At larger bombardment times a stationary value for concentration ratios will be approached which must be considered as representative for the mean bulk composition of the samples.

Finally, it should be noted that surface compositions can be altered due to differences in sputtering yields for different surface constituents. This effect (frequently called "preferential sputtering") depends on the atomic masses and the surface binding energy E_B of the atoms (*25*). For the latter a E_B^{-1} dependence could be established in some cases. Mass dependence arises from the amount of energy that can be transferred between two atoms with masses M_0 and M_s in a single collision and has therefore been discussed in terms of the

transfer factor

$$\gamma = \frac{4M_0M_s}{(M_0 + M_s)^2}. \quad (3)$$

It has been shown for oxides and carbides of heavy metals that this mass effect leads to a pronounced oxygen or carbon depletion, respectively, of the surface under ion bombardment, particularly for light primary particles (He^+) and low energies. The most striking energy dependence occurs at energies below about 10 times the threshold energy E_{th} for sputtering of the heavier component (*26*):

$$E_{th} = \frac{E_B}{\gamma(1 - \gamma)} \quad (4)$$

This effect must certainly be taken into account if signals of lighter elements (O,Al) are evaluated in depth profiling of oxide systems containing heavy metal components (Ni,Mo).

EXPERIMENTAL

Catalyst preparation. Catalysts were prepared as described previously (*13, 15, 16*). The γ-Al_2O_3 support was obtained from the hydroxide (Condea) by calcination in air at 1023 K for 18 h. Its BET surface area was 158 m^2/g. Catalysts were prepared by impregnation (pore-filling method) from aqueous $(NH_4)_6Mo_7O_{24} \cdot 4H_2O$ (puriss.) solutions at pH 6 which contained the requisite amount of molybdate to yield supported catalysts containing 12 wt% MoO_3. The moist material was left overnight (16 h); it was then dried at 393 K for 14 h, and finally calcined at 773 K in air for 2 h. In a second step, $Ni(NO_3)_2$ was impregnated from aqueous solutions containing the requisite amount to yield catalyts with 3 wt% NiO. The drying procedure was analogous to that applied after the first impregnation, while the calcination in air for 2 h was carried out at 573, 673, 773, and 873 K. The catalysts so obtained are designated Ni 3Mo12A1(T), where T indicates the final calcination temperature. The molybdate loading of 12 wt% MoO_3 roughly corresponds to the monolayer capacity of the support material.

Methods. Details of the Raman and diffuse reflectance spectroscopy and of the magnetic susceptibility measurements have been reported previously (*13, 15, 16*).

Ion-scattering experiments were performed in a UHV system (base pressure 10^{-11} mbar) equipped with a cylindrical mirror analyzer with an integrated ion gun (3M Model 515) (*23*). $^4He^+$ ions of 500 eV at a beam current of 4×10^{-8} A were used for analysis and sputter profiling. The ion current density was of the order of magnitude of 10^{-6}A cm^{-2}. A "crater effect" did not occur as shown by using a beam diameter of about 1.4 mm for the ion bombardment and analyzing the central part of the beam spot with a smaller beam of about 0.5 mm diameter, which had a current density lower than that of the bombardment beam by a factor of 10. To avoid any charging effects of the insulating catalysts which would distort the energy spectra, the specimens were flooded with thermal electrons. No effect on the ion neutralization, i.e., peak heights, was observed when this technique was applied.

To remove any surface contaminations, samples were exposed to an O_2 beam ($\sim 10^{-4}$ mbar) at approximately 500 K prior to the final evacuation. This procedure allowed well-resolved, good quality energy spectra to be recorded.

RESULTS AND DISCUSSION

Raman Spectroscopy

Raman spectra of the four samples calcined at temperatures between 570 and 870 K are shown in Fig. 1. All spectra exhibit the previously reported features which are characteristic of the proposed surface polymolybdate structure (*13, 27–30*). The sharp band at 1052 cm^{-1} observed in the spectrum of Ni3Mo12A1(570) is to be assigned as a normal mode of the NO_3^- anion, indicating that this species is not quantitatively decomposed at 570 K. No evidence

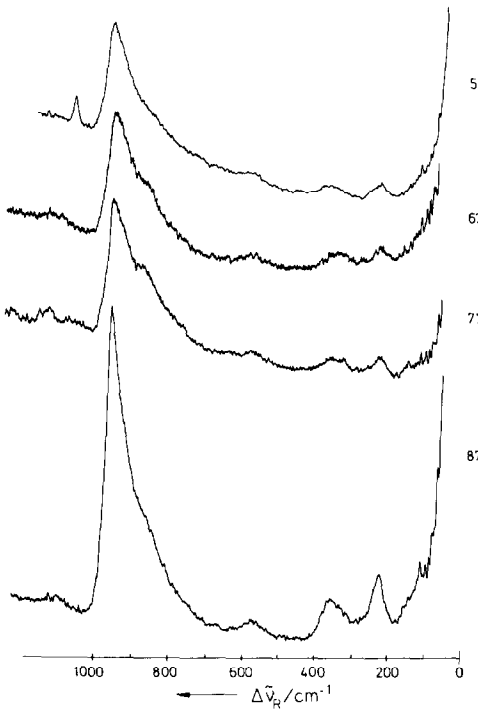

FIG. 1. Raman spectra of Ni3Mo12Al catalysts and their dependence on catalyst calcination temperature.

for the formation of MoO_3, $NiMoO_4$, or $Al_2(MoO_4)_3$ at detectable levels is seen in the spectra.

Spectra of the samples calcined at temperatures up to 770 K are very similar regarding band positions, band widths, and intensities. In contrast, in the spectrum of Ni3Mo12Al(870) the bands at 220 cm^{-1} (Mo–O–Mo deformation) and at 950 cm^{-1} (Mo=O symmetric stretching) sharpen and have considerably enhanced intensity. In addition, the usually weak feature at 569 cm^{-1} (symmetric Mo–O–Mo stretching) is much more clearly developed than at lower calcination temperature. The polymolybdate phase has been described (*13, 29*) as a surface analog of nickel heteropolymolybdates, which is built up by edge-sharing MoO_6 octahedra. In this structure the Ni^{2+} ions should be located in octahedral sites. It has to be assumed that the MoO_6 octahedra in strong chemical interaction with the support surface are irregularly distorted. This distortion must be responsible for the large width of the Raman bands as compared to solution spectra, and for the presumably relatively low scattering cross-sections. The sharpening of the bands and their enhanced intensities (probably due to increased scattering cross sections) on calcination at 870 K must then indicate some structural reorganization which leads to polymeric species with less distorted MoO_6 octahedra. In addition, a better spreading of the molybdate layer might also be considered responsible for this phenomenon.

Diffuse Reflectance Spectroscopy (DRS)

The appearance of a very intense ligand charge-transfer (LCT) band at 300 nm in all samples confirms the formation of a polymolybdate surface phase (*30*). Most typically Ni^{2+} in octahedral environment gives rise to a ligand field transition near 400 nm (*31*) which is assigned as the O_3 band ($^3A_{2g} \rightarrow {}^3T_1(P)$). This band is strongly overwhelmed by the LCT band and, if at all, it can only be detected as a weak shoulder. The characteristic absorption of Ni^{2+} in tetrahedral oxygen environment leads to a spin-orbit split t_3 band ($^3T_1 \rightarrow {}^3T_1(F)$) near 600 nm. In nickel aluminates this doublet appears at 575 and 612 nm (*16, 31, 32*). Figure 2 shows the DR spectra of variously calcined catalysts in the wavelength region 450 to 700 nm. Very clearly, absorption bands near 600 nm cannot be detected at the low calcination temperatures suggesting the absence of Ni^{2+} in tetrahedral coordination at a detectable level. The Ni^{2+} ions should therefore be located in octahedral sites of the surface polymolybdate and perhaps in the support spinel matrix. When the calcination temperature is raised to above 770 K the t_3 doublet develops with increasing intensity. In agreement with previous results (*13, 15, 16*), the increased tetrahedral site population is most probably to be attributed to a penetration of Ni^{2+} ions from the surface phase into the support matrix, which process is expected to become more pronounced at the higher calcination tem-

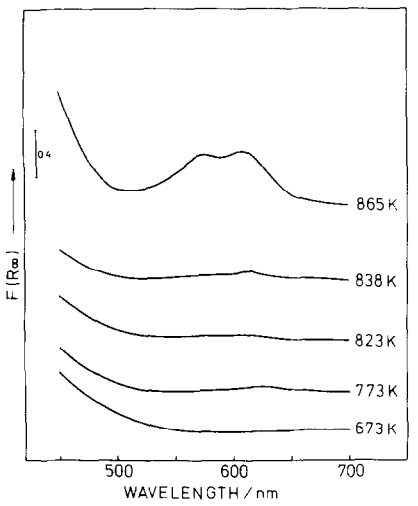

FIG. 2. Diffuse reflectance spectra of Ni3Mo12Al catalysts and their dependence on catalyst calcination temperature.

peratures. These conclusions are strongly supported by the fact that the magnetic susceptibilities of these catalysts clearly increase with increasing calcination temperature.

Ion-Scattering Spectroscopy

The above physical characterization of the catalysts suggests the formation of a more or less well spread surface polymolybdate layer (perhaps a monolayer), the homogeneity of which seems to improve at calcination temperatures above 770 K. Simultaneously, the Ni^{2+} ions tend to penetrate from the surface into the support matrix. Hence, depending on calcination temperature the exposure of Mo and Al in the topmost atomic layers should vary and the surface Ni/Mo ratio should significantly decrease as Ni^{2+} diffuses into the bulk. These effects should very clearly show up in the ion scattering spectra.

Figures 3 and 4 show typical energy spectra as they develop with increasing bombardment time for samples that had been calcined at 773 K (Fig. 3) and at 573 and 873 K (Fig. 4). Experiments of this type have been carried out repeatedly using different areas of the specimen surface and identical

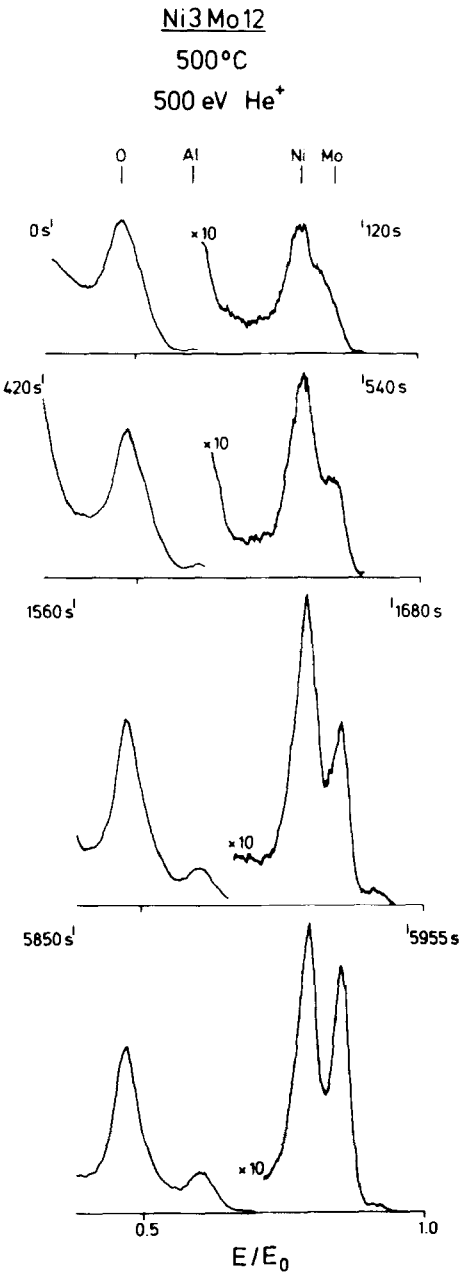

FIG. 3. Ion-scattering spectra of catalyst Ni 3Mo12Al(770) as they develop with increasing bombardment time.

general trends have been obtained in each case. Hence, the spectra are representative for the overall catalyst sample. The signals of O, Al, Ni, and Mo are clearly detected in the spectra of Figs. 3 and 4 and the peak intensities at the maximum can be mea-

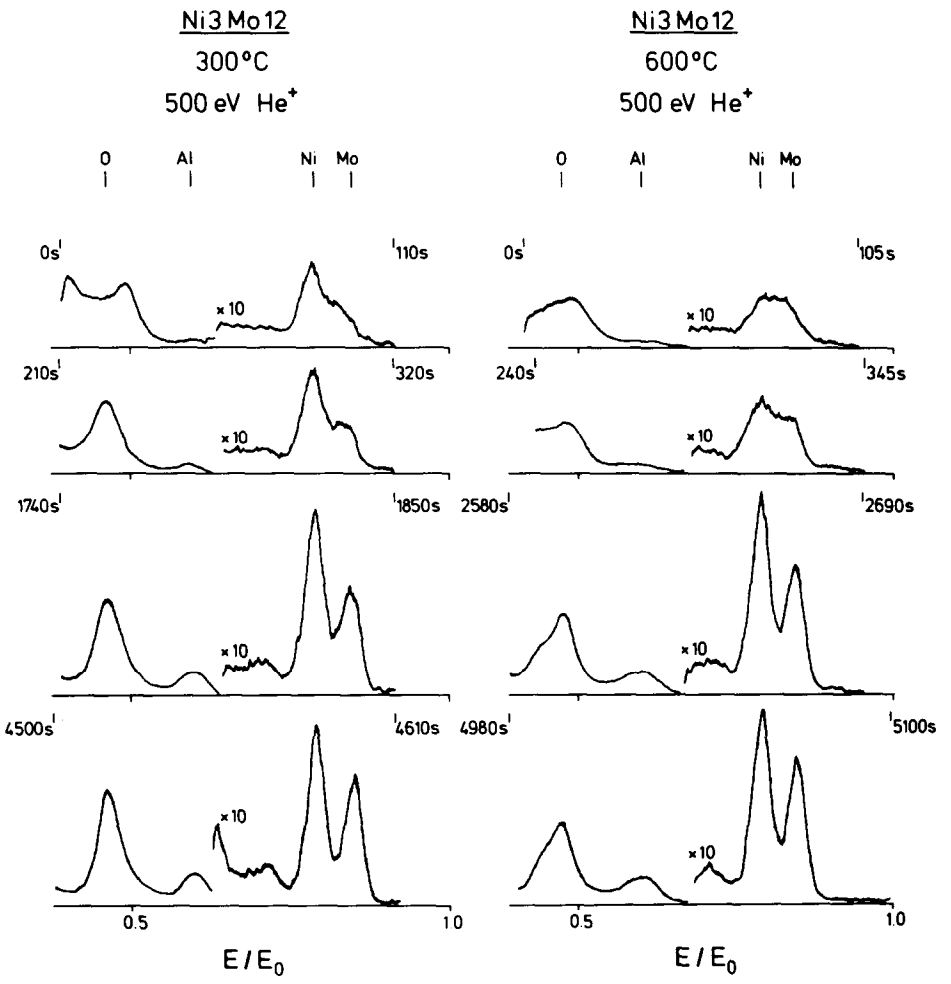

FIG. 4. Ion-scattering spectra of catalysts Ni3Mo12Al(570) and Ni3Mo12Al(870) as they develop with increasing bombardment time.

sured for the determination of intensity ratios. The Ni/Mo intensity ratios are not affected by preferential sputtering since the transfer factors (Eq. (3)) are essentially the same for both elements. The transfer factor for Al on the other hand is higher by a factor of approximately 2 which can lead to a relative enrichment of the heavier elements Ni and Mo with increasing sputtering time.

At the applied current density of 10^{-6} A cm^{-2} and assuming a sputter yield of 10^{-1} atoms per ion at 500 eV (*33*), one estimates a time of approximately 17 to 34 min to remove a monolayer. Due to the angular dependence of the sputter yield, these values can only be a rough estimate for the erosion time of one monolayer.

Figure 5 represents depth profiles for the Mo/Al intensity ratios of the catalysts Ni 3Mo12Al(570), Ni3Mo12Al(770), and Ni 3Mo12A1(870). For the first two of these catalysts the Mo/Al ratio clearly has a finite initial value at zero bombardment time indicating the nonzero abundance of Al in the surface layer of the catalysts. This suggests the exposure of free uncovered support areas and of the presence of at least certain patches of three-dimensional molybdate surface species, since the total loading corresponds to the theoretical monolayer ca-

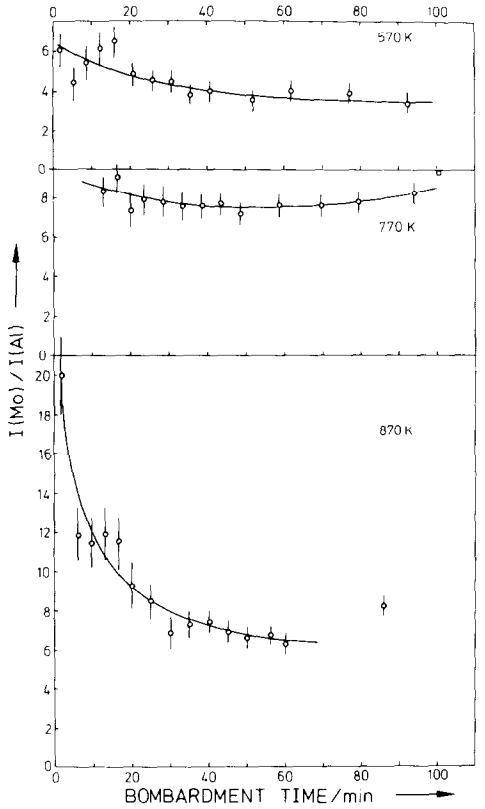

FIG. 5. ISS intensity ratios Mo/Al as a function of bombardment time ("depth profiles") for catalyst Ni 3Mo12Al calcined at 570, 770, and 870 K.

pacity. The higher initial Mo/Al intensity for Ni3Mo12Al(770) indicates an improved dispersion of the molybdate layer as compared to catalyst Ni3Mo12Al(570). The slight increase of this ratio at large bombardment times must be due to the preferential sputtering of Al.

In contrast to samples calcined at temperatures up 770 K, the Mo/Al intensity ratio has a very high value at low bombardment times for catalyst Ni3Mo12Al(870). It is inferred, therefore, that an increased mobility of surface molybdate species at 870 K leads to a reorganization of the surface molybdate layer, which must be accompanied by a spreading over the support surface and an improved monolayer formation. It should be noted that the dramatic changes of the Mo/Al ratio before the stationary value is reached occur in a time period of 35 to 40 min, which corresponds approximately to the removal of one or two monolayers. It must also be stressed that these trends were also detected in the Raman spectra, as discussed above.

Hence, samples calcined at temperatures below 770 K should expose islands of uncovered support surface and a surface molybdate layer which must exhibit at least locally a three-dimensional expansion. Since Raman spectroscopy did not detect any MoO_3 or other bulk compounds, these three-dimensional surface molybdates may develop structures comparable to those of polyanions having edge-bridging MoO_6 octahedra in two superimposed layers. These conclusions are in agreement with arguments put forward by Cirillo *et al.* (*34*) on the basis of ^{1}H-NMR experiments, from which clustering of Al-OH groups into areas not covered by molybdena was assumed.

It had been shown previously (*15*) that the Ni distribution between molybdate layer and support is sensitively influenced by the calcination time at 770 K. Therefore, a strong effect of the calcination temperature on the Ni/Mo intensity ratios should be expected. Figure 6 shows the respective depth profiles for the catalysts Ni 3Mo12Al(570), Ni3Mo12Al(770), and Ni 3Mo12Al(870). In all cases the final steady state values seem to be approximately identical and typical for the overall composition of the catalysts. The depth profile of catalyst Ni3Mo12Al(570) has a high initial value for the Ni/Mo ratio which then drops fairly steeply with increasing bombardment time. However, this profile is perhaps not typical for this type of catalyst since $Ni(NO_3)_2$ is not quantitatively decomposed at 570 K, as shown above by means of Raman spectroscopy. After calcination at 770 K the initial Ni/Mo value is lower and shows the typical falling trend which had already been reported previously (*13, 15, 16*) for the same calcination conditions. However, this trend is reversed after calcination at 870 K (see Fig. 6) where the Ni/

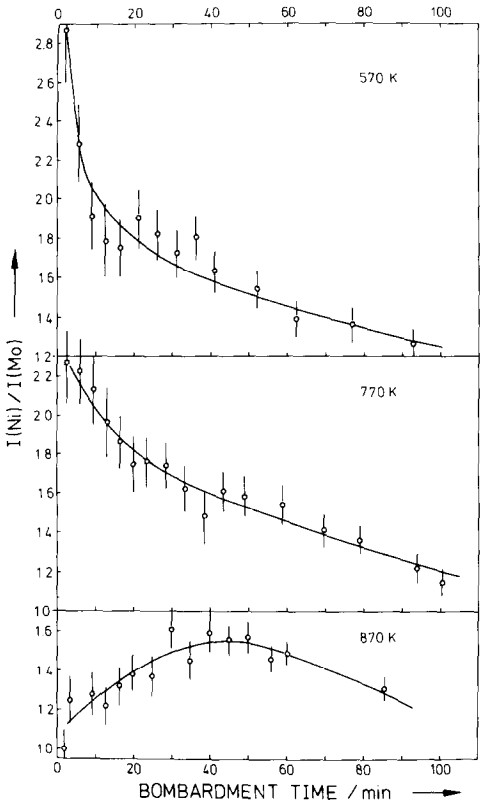

FIG. 6. ISS intensity ratios Ni/Mo as a function of bombardment time ("depth profiles") for catalyst Ni 3Mo12Al calcined at 570, 770, and 870 K.

Mo ratios are low at zero bombardment time and then rise and pass through a flat maximum after 40 to 50 min bombardment time. The finite value of the Ni/Mo ratio at zero bombardment time suggests that Ni must still be exposed in the topmost atomic layer although the molybdate should now have formed a relatively well-developed monolayer covering the support surface. Hence, the Ni^{2+} ions must be incorporated within the molybdate layer.

The temperature dependence of these depth profiles clearly shows that the relative Ni^{2+} concentration in the surface layer is reduced with increasing calcination temperature due to diffusion of the Ni^{2+} into the support lattice where it forms a surface spinel with Ni^{2+} in octahedral *and* tetrahedral positions in agreement with the above mentioned optical spectroscopic and magnetic results.

CONCLUSIONS

Regarding the ISS technique, the described experiments and results certainly demonstrate the potential usefulness of this technique for the characterization of real catalyst surfaces, i.e., of high surface area dispersed and porous materials. This is specifically supported here by the simultaneous application of other physical techniques. It must, however, also be emphasized that depth profiles can only be interpreted as qualitative trends, since a homogeneous layer-by-layer erosion on rough surfaces is impossible.

Regarding the structure of the supported NiMo catalysts, the following conclusions can be drawn:

1. At calcination temperatures $T \leq 770$ K, the molybdate surface layer is nonhomogeneous, and consists most probably of patches which are composed of a varying number of layers of edge-sharing MoO_6 octahedra. These structures might be analogous to the structures of poly or heteropolymolybdates. Besides these molybdate patches, uncovered Al_2O_3 support surface must be exposed.

2. Calcination at 870 K leads to a spreading of the molybdate over the Al_2O_3 surface and forms probably a two-dimensional monolayer of edge-sharing MoO_6 octahedra. In this situation, the octahedra seem to be much less distorted than for the samples calcined at lower temperature.

3. The Ni^{2+} promoter ions are partially incorporated in the surface molybdate layer, where they occupy octahedral coordination sites.

4. The distribution of the Ni^{2+} between the molybdate layer and the support spinel matrix depends very strongly on the sequence of impregnation (*13*), the calcination time (15) as shown previously, and very clearly on the calcination temperature as demonstrated by the present results. Hence, the surface Ni/Mo ratio can be controlled by these parameters in the oxide precursor state.

5. These results have some important relevance with respect to the catalyst performance after a given pretreatment since the hydrogenation/hydrodesulfurization selectivity depends on the surface Ni/Mo ratio (*13*). Also, the results suggest that this type of catalyst must be regenerated under mild enough conditions, so that the surface composition remains unchanged during regeneration.

ACKNOWLEDGMENTS

This work was financially supported by the Deutsche Forschungsgemeinschaft and the Fonds der Chemischen Industrie.

REFERENCES

1. Smith, D. P., *Surf. Sci.* **25,** 171 (1971); Smith, D. P., *J. Appl. Phys.* **38,** 340 (1967).
2. Heiland, W., and Taglauer, E., *Nucl. Instrum. Methods* **132,** 535 (1976).
3. Brongersma, H. H., and Buck, T. M., *Nucl. Instrum. Methods* **132,** 559 (1976).
4. Shelef, M., Wheeler, M. A. Z., and Yao, H. C., *Surf. Sci.* **47,** 697 (1975).
5. Brongersma, H. H., Beirens, L. C. M., and van der Ligt, G. C. J., *in* "Material Characterization Using Ion Beams" (J. P. Thomas, and A. Cachard, Eds.), p. 65. Plenum, New York, 1978.
6. Wu, M., and Hercules, D. M., *J. Phys. Chem.* **83,** 2003 (1979).
7. Chin, R. L., and Hercules, D. M., *J. Phys. Chem.* **86,** 360 (1982).
8. Chin, R. L., and Hercules, D.M., *J. Catal.* **74,** 121 (1982).
9. Zingg, D. S., Makovsky, L. E., Tischer, R. E., Brown, F. R., and Hercules, D. M., *J. Phys. Chem.* **84,** 2898 (1980).
10. Delannay, F., Haeussler, E. N., and Delmon, B., *J. Catal.* **66,** 469 (1980).
11. Delannay, F., and Defossé, C., *Amer. Chem. Soc. Div. Petr. Chem. Prepr.* **26,** 385 (1981).
12. Gajardo, P., Grange, P., and Delmon, B., *J. Catal.* **63,** 201 (1980).
13. Knözinger, H., Jeziorowski, H., and Taglauer, E., "Proceedings, International Congress on Catalysis, 7th (Tokyo 1980)," p. 604. Elsevier–Kodansha, Amsterdam/Tokyo, 1981.
14. Knözinger, H., and Taglauer, E., *Amer. Chem. Soc. Div. Petr. Chem. Prepr.* **26,** 357 (1981).
15. Canosa Rodrigo, B., Jeziorowski, H., Knözinger, H., Wang, X. Sh., and Taglauer, E., *Bull. Soc. Chim. Belg.* **90,** 1339 (1981).
16. Abart, J., Delgado, E., Ertl, G., Jeziorowski, H., Knözinger, H., Thiele, N., Wang, X. Sh., and Taglauer, E., *Appl. Catal.* **2,** 155 (1982).
17. Taglauer, E., and Heiland, W., *Appl. Phys.* **9,** 261 (1976).
18. Firsov, O. B., *Sov. Phys. JETP* **36,** 1076 (1959).
19. Heiland, W., Taglauer, E., and Robinson, M. T., *Nucl. Instrum. Methods* **132,** 655 (1976).
20. Wilson, K., Haggmark, L., and Biersack, L., *Phys. Rev. Sect. B* **15,** 2458 (1980).
21. Taglauer, E., and Heiland, W., *Surf. Sci.* **47,** 234 (1975).
22. Rusch, T. W., McKinney, J. T., and Leys, J. A., *J. Vac. Sci. Technol.* **12,** 400 (1975).
23. Taglauer, E., Heiland, W., and Onsgaard, J., *Nucl. Instrum. Methods* **168,** 571 (1980).
24. Bay, H. L., and Bohdansky, J., *Appl. Phys.* **19,** 421 (1979).
25. Taglauer, E., Heiland, W., and McDonald, R., *Surf. Sci.* **90,** 661 (1979).
26. Bohdansky, J., Roth, J., and Bay, H., *J. Appl. Phys.* **51,** 2861 (1980).
27. Payen, E., Dhamelincourt, M. C., Dhamelincourt, P., Grimblot, J., and Bonnelle, J. P., *Appl. Spectrosc.* **36,** 30 (1982).
28. Dufresne, P., Payen, E., Grimblot, J., and Bonnelle, J. P., *J. Phys. Chem.* **85,** 2344 (1981).
29. Jeziorowski, H., and Knözinger, H., *Appl. Surf. Sci.* **5,** 335 (1980).
30. Jeziorowski, H., and Knözinger, H., *J. Phys. Chem.* **83,** 1166 (1979).
31. Reinen, D., *Struct. Bonding (Berlin)* **7,** 114 (1970).
32. LoJacono, M., Schiavello, M., and Cimino, A., *J. Phys. Chem.* **75,** 1044 (1971).
33. Roth, J., Bohdansky, J., and Ottenberger, W., Report-IPP 9/26 (1979) of the Max Planck Institut für Plasmaphysik.
34. Cirillo, Jr., A. C., Dollish, F. R., and Hall, W. K., *J. Catal.* **62,** 379 (1980).